Biochimica et Biophysica Acta, 357 (1974) 67–77

BBA 46758

REACTION CENTER BACTERIOCHLOROPHYLL TRIPLET STATES: REDOX POTENTIAL DEPENDENCE AND KINETICS

JOHN S. LEIGH Jr and P. LESLIE DUTTON

Johnson Research Foundation, University of Pennsylvania, Philadelphia, Pa. 19174 (U.S.A.)

(Received October 1st, 1973)
(Revised manuscript received March 27th, 1974)

SUMMARY

Triplet states of reaction center (bacterio-) chlorophylls have been observed by low temperature EPR in a wide variety of photosynthetic preparations ranging from whole cells to purified reaction centers. The reaction center triplet state is seen under conditions where electron transfer from the reaction center chlorophyll is prevented by reduction of the primary electron acceptor. The redox potential dependence shows one-electron titrations with midpoint potentials of -50 mV in *Rhodopseudomonas spheroides* and approx. -120 ± 20 mV in *R. rubrum* and *Chromatium* D. Kinetic measurements with bacterial reaction centers show an approx. 6-μs triplet decay time. Observed zero-field splitting parameters D and E are appreciably lower in the reaction center triplets than in isolated chlorophyll, suggesting that the reaction center photo-active (bacterio-) chlorophyll is not monomeric. EPR lineshapes of the triplet signals (equal mixtures of microwave absorption and emission) show almost complete spin polarization demonstrating that inter-system crossing is a highly selective process.

INTRODUCTION

The possible role of chlorophyll and bacteriochlorophyll triplet states in primary events of photosynthesis is an old and interesting problem. The implication of chlorophyll triplet states in vitro as intermediates in photochemistry is well established [1, 2]. This has led to much speculation concerning the possible role of chlorophyll triplet states in vivo [3–5]. Attempts to study the triplet state in intact photosynthetic systems have been hampered by the lack of direct or reliable monitors of chlorophyll and bacteriochlorophyll triplet populations. This paper describes low-temperature EPR characteristics of triplet states in photosynthetic bacteria which are associated with the reaction center bacteriochlorophyll [6, 7].

Optical characteristics of chlorophyll and bacteriochlorophyll triplet states in organic solvents have been studied by flash photolysis techniques [8, 9]. Quantum yields of triplet state formation as high as 90–100 % have been observed [1, 10, 11]. Luminescence associated with the triplet states of chlorophylls *a* and *b* has also been

observed from purified green plant chlorophyll solutions [12]. As far as is known, no unequivocal observations of triplet phosphorescence in bacteriochlorophyll derived from photosynthetic bacteria has ever been detected. Energy transfer studies have shown that the lowest bacteriochlorophyll triplet state lies lower than 7700 cm^{-1} [11]. There have been suggestions, however, that the longest lived chlorophyll triplet state may well not be the lowest lying, but, rather, the second excited triplet level [13].

Electron paramagnetic resonance techniques have proved to be an excellent and generally unequivocal method to detect triplet states in many cases. Analysis of EPR lineshape provides a measure of so-called zero-field splitting parameters. These zero-field splitting parameters are caused by spin–spin interaction between the two electron orbitals associated with the particular triplet state and are sensitive indicators of the average spatial geometry of the orbitals.

EPR signals of triplet states in purified chlorophyll were first observed by Azizova et al. [14]. Lhoste [15] has characterized the EPR spectra of triplet states of purified chlorophylls *a* and *b* in ethanol at liquid nitrogen temperatures. The lineshapes of these signals were analyzed to give zero-field splitting parameters $D = 306 \cdot 10^{-4}$ cm^{-1} and $E = 34 \cdot 10^{-4}$ cm^{-1}. Similar zero-field splitting values have been obtained for zinc prophin by optically detected magnetic resonance techniques [16]. A triplet EPR signal from chromatophore and subchromatophore preparations of *Chromatium* D [6] and from reaction center preparations of *Rhodopseudomonas spheroides* [7] has been previously described. The signal was identified with the triplet state of reaction center bacteriochlorophyll primarily from the fact that it was apparent only upon reduction of the primary electron acceptor. The unusual lineshape of the signal was ascribed to a combination of EPR absorption and emission. This situation may be caused by a phenomenon which has been called spin polarization, and has been previously observed in organic single crystals.

Triplet state EPR

The spin hamiltonian of the bacteriochlorophyll triplet state may be written in the general form:

$$\mathscr{H} = \mathscr{H}_{\boldsymbol{H}} + \mathscr{H}_{SS} + \mathscr{H}_{SO}$$

where $\mathscr{H}_{\boldsymbol{H}} = \beta \boldsymbol{H} \cdot g \cdot S$ is the usual Zeeman interaction of the total electron spin $S = S_1 + S_2$ with the applied magnetic field $\boldsymbol{H}$. $\mathscr{H}_{SS}$ is the spin–spin interaction and includes both dipolar and exchange contributions. $\mathscr{H}_{SO}$ is the spin–orbit interaction. In magnetic fields of approx. 3000 G (X-band EPR) $\mathscr{H}_{\boldsymbol{H}}$ is approx. 0.3 cm^{-1}. Estimates for the magnitude of the exchange part of the spin–spin interaction terms are not easily available. Dipolar interaction of two electrons at 4 Å distance represents an energy of approx. 0.03 cm^{-1}.

It is convenient to cast the spin hamiltonian into its usual simplified form:

$$\mathscr{H} = g\beta \boldsymbol{H} \cdot S + D(S_Z^2 - 2/3) + E(S_x^2 - S_y^2)$$

in which we have assumed an isotropic g value. All of the anisotropic spin–spin interactions have been combined to give the phenomenologically measurable zero-field splitting parameters D and E. The basic spin functions appropriate for large magnetic fields include three symmetric (triplet) states:

$|\alpha_1\alpha_2\rangle$, $1/\sqrt{2}\,(|\alpha_1\beta_2\rangle + |\beta_1\alpha_2\rangle)$, $|\beta_1\beta_2\rangle$

which may be conveniently labeled by their Z components T_{+1}, T_0 and T_{-1}, respectively, and the antisymmetric (singlet) spin function $S^* = 1/\sqrt{2}\,(|\alpha_1\beta_2\rangle - |\beta_1\alpha_2\rangle)$.

The EPR lineshape of randomly oriented triplet state molecules has been described by Wasserman et al. [17]. There are three possible transitions among the triplet levels. The most prominent feature of the majority of triplet spectra is an (almost) isotropic line at approx. g 4, which corresponds to the transition $T_{+1} \leftrightarrow T_{-1}$, the so-called $\Delta M = 2$ transition. For small zero-field splitting values, each of the two $\Delta M = 1$ transitions ($T_{+1} \leftrightarrow T_0$ and $T_0 \leftrightarrow T_{-1}$) are symmetrically located around the g 2 region. The anisotropy of the zero-field splittings, in general, leads to six $\Delta M = 1$ EPR "lines". Assuming that D is positive, the $T_{+1} \leftrightarrow T_0$ transition has z, y, and x components at fields which are displaced from the center ($g = 2.0$) by amounts $-D$, $-(D-3E)/2$ and $+(D+3E)/2$, respectively. Correspondingly, the $T_0 \leftrightarrow T_{-1}$ transition has lines at positions displaced by $+D$, $-(D-3E)/2$ and $-(D+3E)/2$ from the center. A computer simulation of the composite lineshape of the $\Delta M = 1$ transition with D and E values chosen appropriate to the bacteriochlorophyll reaction center triplet is shown in Fig. 1A. This simulation assumes that thermal (Boltzmann) equilibrium exists between the spin states within the triplet manifold.

The matrix elements which cause singlet–triplet mixing couple together the S^* (excited) singlet state only with the T_0 triplet state. This is true for both spin–orbit and exchange interactions [16, 18]. The T_{+1} and T_{-1} levels are not mixed with the singlet state by static interactions. Thus, one expects entry into the triplet state from

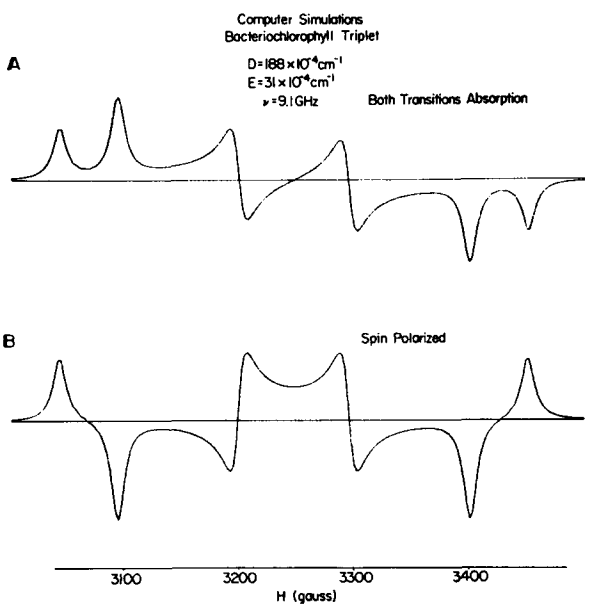

Fig. 1. Computer triplet EPR spectra. (A) X-band EPR lineshape for a triplet state with zero-field splitting parameters $D = 188 \cdot 10^{-4}$ cm^{-1} and $E = 31 \cdot 10^{-4}$ cm^{-1}. Both $T_{-1} \leftrightarrow T_0$ and $T_0 \leftrightarrow T_1$ transitions are assumed to be normal derivative Lorentzian absorption lines with a width of 15 G. (B) Same as upper (A) spectrum except the $T_0 \leftrightarrow T_{-1}$ transition was calculated as an emission.

the excited singlet state (intersystem crossing) to be highly spin selective. At early times, only the T_0 triplet level would be populated. Spin-lattice relaxation (presumably effected by thermal fluctuations of zero-field splitting) would operate to distribute the spins between the other (T_{+1} and T_{-1}) triplet levels at a rate determined by the spin-lattice relaxation time. The lifetime(s) of the triplet state are governed by the phosphorescence and internal conversion rates.

The EPR lineshape of randomly oriented spin-polarized triplet states should be similar to that of "normal" (thermally equilibrated) triplet states, except that one of the $\Delta M = 1$ transitions should occur as microwave emission rather than absorption. The $\Delta M = 2$ line should be absent due to the low and equal population of the T_{+1} and T_{-1} triplet levels. A computer simulation of such a situation is shown in Fig. 1B with identical zero-field splitting parameters to that in Fig. 1A.

Spin polarization of excited triplet states in organic crystals have been studied optically [19, 20] and by EPR techniques [21].

METHODS

Various species of photosynthetic bacteria (*Chromatium* D; *R. rubrum*; blue-green mutant strain G 9; *Rps. spheroides*; blue-green mutant R 26, or the green mutant Ga; and *Rhodospseudomonas gelatinosa*, strain I) were grown anaerobically in the light on succinate as sole carbon source. Chromatophores were prepared by the alumina grinding method described by Baltscheffsky [22] or by sonication [24] from 1–2-day-old cultures. Both methods gave equivalent results. *Chromatium* D subchromatophore particles (Fraction A and Fraction B) were prepared by the sodium dodecylsulfate–Thornber technique [23]. Bacteriochlorophyll was assayed in vivo spectrophotometrically at the relevant peaks in the 590-nm region, using an extinction coefficient of 20 $mM^{-1} \cdot cm^{-1}$. Subchromatophores of *Rps. spheroides* Ga (containing reaction centers) were prepared by exposing chromatophores to 3 % Triton X-100 with subsequent purification by Biogel column chromatography. Reaction centers from *Rps. spheroides* R26 were prepared from chromatophores using 1 % *N*-lauryl-*N*, *N*-dimethylamine-*N*-oxide (Onyx Chemical Co., Jersey City, New Jersey) as previously described [7].

Redox potentiometry was performed as previously described [24]. A Varian E-3 EPR spectrometer equipped with a flowing helium cryostat (Air Products, Allentown, Pa.) was used for EPR measurements. In order to obtain rapid kinetic traces, the 100 KHz magnetic field modulation normally used to obtain ESR spectra was disabled. The AFC modulation was adjusted to a minimum usable level. Signals were taken directly from the microwave bridge and displayed on a high speed storage oscilloscope. Response times of about 500 ns which were almost artifact-free were achieved. This type of signal detection gives the kinetics of the EPR absorption signal instead of the more conventional first derivative presentation.

Steady-state sample illumination in the microwave cavity at cryogenic temperatures was provided by filtered light from a focused 40 W Unitron Lamp. Wratten 88A filters and a 2-cm water filter were used to isolate a relatively broad band of infrared light. Flash illumination for kinetic studies was provided by a tunable liquid dye laser (Rhodamine 6G) operated at approx. 590 nm, which emitted flash energies of about 100 mJ and a full width at half height of approx. 500 ns. Computer

simulations of EPR lineshapes were done with a PDP-10 computer and CalComp plotter at the University of Pennsylvania, Medical School Computer Facility.

RESULTS

Triplet EPR signals

Illumination of samples in which electron transfer from reaction center bacteriochlorophyll is blocked, leads to a readily detectable accumulation of bacteriochlorophyll triplet state. A typical EPR spectrum of the photo-induced signals at redox potentials at which the primary acceptor is reduced (i.e. below −100 mV) in *Rps. spheroides* (R26) mutant reaction center particles is shown in Fig. 2. The spectrum was taken with steady-state illumination and EPR spectrometer conditions set to produce the normal first derivative presentation of an absorption line. The unusual lineshape shows a mixture of EPR absorption and emission signals. The correspondence of peak positions and similarity of relative lineshape features between the computer-simulated spectrum shown in Fig. 1B, and the low-potential photo-induced signal leaves little doubt that the EPR signal in Fig. 2 is, in fact, a spin-polarized triplet state. No $\Delta M = 2$ line at approximately g 4 was observed. Fig. 3 shows the triplet signal obtainable from a suspension of whole cells of *Rps. spheroides*, demonstrating that the visualization of the effect was not the result of preparative artifacts. Analogous spin-polarized triplet signals were easily seen in every photosynthetic bacterium examined.

A compilation of calculated zero-field splitting parameters (D and E) is shown in Table I. It is interesting that even though rather large differences in D and E values exist between different bacteria, all active preparations from the same bacterium give virtually identical results. The last digit of the parameters shown is numerically significant and differences of $1 \cdot 10^{-4}\,cm^{-1}$ are comfortably outside experimental error on a relative comparison basis, however, absolute precision may be as poor as 5 % due to uncertainties in the absolute scale of magnetic field.

A similar, though much weaker signal, which probably represents the triplet state of the reaction center chlorophyll in Photosystem I particles from spinach is

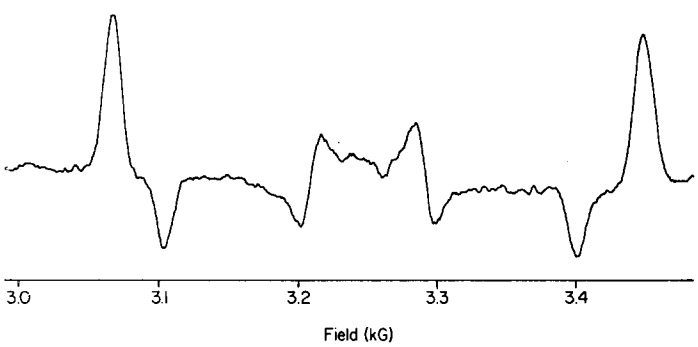

Fig. 2. Photo-induced triplet EPR signal from *Rps. spheroides* (R26) reaction centers. Sample containing 90 μM reaction centers in 0.1 % Triton X-100, 20 mM MOPS–NaOH, pH 7.2, was reduced with $Na_2S_2O_4$, and illuminated with infrared light. Temperature 8 °K, at a microwave power of 20 mW.

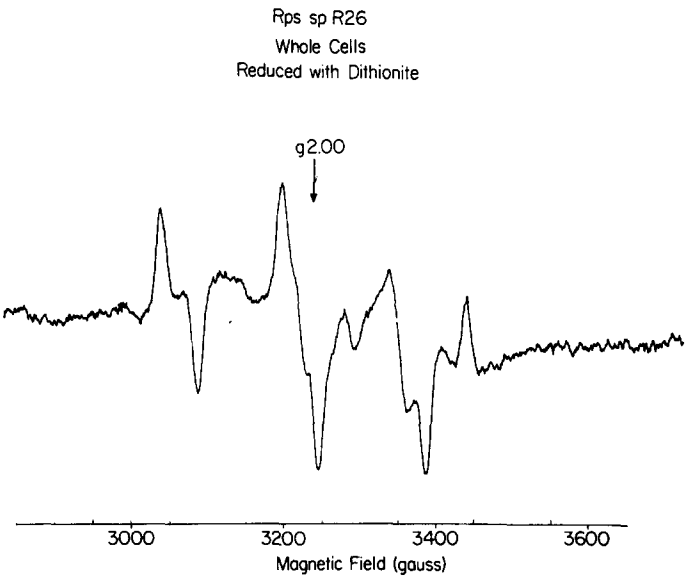

Fig. 3. Photo-induced triplet EPR signal from *Rps. spheroides* (R26), whole cells. Sample of whole cells at a bacteriochlorophyll concentration of 2 mM was suspended in 20 mM Tris–Cl^-, pH 7.8, and reduced with $Na_2S_2O_4$. Other conditions as in Fig. 2. In addition to the prominent triplet lines, free radical signals at g 2.00 and iron–sulfur protein signals at g 2.03 and 1.94 are also evident.

TABLE I

	D (cm^{-1}) ($\times 10^4$)	E (cm^{-1}) ($\times 10^4$)
Reaction center preparations		
Rps. spheroides R26	188	31
Rps. spheroides R26 (in lecithin)	188	31
Rps. spheroides R26 (after sodium dodecylsulfate) ref. 31	188	32
Rps. spheroides Ga (subchromatophore particles)	161	27
Chromatium D (sodium dodecylsulfate subchromatophore particles)	178	33
Chromatophores		
R. rubrum blue-green mutant	162	28
R. rubrum blue-green mutant in 60 % glycerol	162	28
Chromatium D	178	33
Rps. spheroides Ga	159	26
Rps. gelatinosa	158	24
Whole cells		
Rps. spheroides R26	188	31

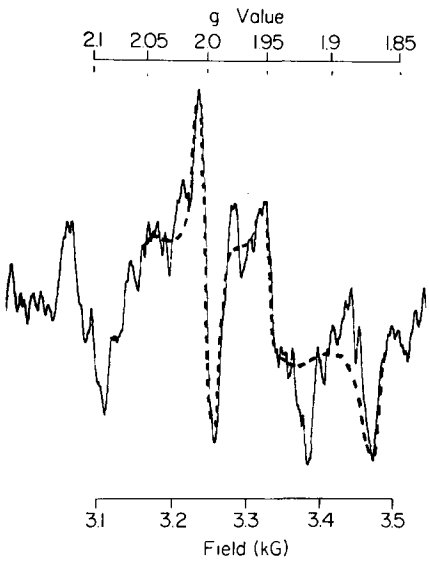

Fig. 4. Photo-induced triplet EPR signal from spinach Photosystem I particles. Sample of Photosystem I particles was prepared from spinach chloroplasts by Triton X-100 treatment and $(NH_4)_2SO_4$ fractionation. Partially reduced sample was illuminated with white light in the EPR cavity at 8 °K. Spectrum was accumulated on a computer as the summation of 25 scans in the light minus 25 scans in the dark. Dashed line approximates baseline variation caused by light-induced heating of the sample. Temperature, 10 °K; microwave power, 1 mW.

shown in Fig. 4. Approximate zero-field splitting parameters are $D = 154 \cdot 10^{-4}$ cm^{-1} and $E = 25 \cdot 10^{-4}$ cm^{-1}.

Redox potential dependence

The dependence on redox potential (established prior to freezing) of the light-induced extent of both reaction center triplet (^{3}BChl) and reaction center

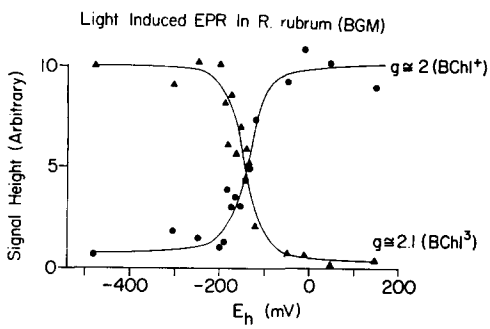

Fig. 5. Redox potential dependence of bacteriochlorophyll photo-oxidation and photo-induced triplet signals in *R. rubrum* (blue-green mutant) chromatophores. The following mediators were used to establish known redox potentials of samples prior to freezing: diaminodurene, 50 μM; phenazine methosulfate, 40 μM; phenazine ethosulfate, 40 μM; pyocyanine, 40 μM; 2-hydroxy-1,4-naphthaquinone, 100 μM; anthraquinone-2-sulfonate, 100 μM; anthraquinone-2,6-sulfonate, 400 μM; benzyl and methyl viologen, 50 μM each.

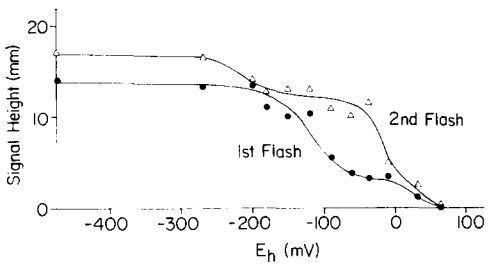

Fig. 6. Redox potential dependence of flash-induced triplet EPR signal in *Chromatium* D. Chromatophores from *Chromatium* D at a bacteriochlorophyll concentration of 1.8 mM were redox poised in the dark (as in Fig. 5), and the flash-induced triplet EPR signal was assayed at its maximum at a temperature near 8 °K. Liquid dye laser at 590 nm was used for flash illumination.

oxidation ($BChl^+$) in a sample of *R. rubrum* (blue-green mutant) chromatophores is shown in Fig. 5. It is clear that in the steady state, the formation of ^3BChl and $BChl^+$ are mutually exclusive. Both reflect the redox midpoint potential of the primary electron acceptor showing an apparent midpoint potential of -120 mV, a value which agrees with that measured by Cramer [25].

In *Rps. spheroides*, midpoint values of -50 ± 20 mV at pH 7.2 are obtained from chromatophores of the carotenoid-deficient Ga mutant, and from reaction centers of the carotenoid-free mutant, R26. Again, the midpoint obtained indicates that the light-induced triplet state, as is the level of light-induced oxidation, is controlled by the state of reduction of the primary acceptor.

The proposal that the level of photo-inducable triplet signal is indicative of the state of reduction of the primary electron, is strongly supported by the redox potential dependence of flash-induced triplet EPR signals in *Chromatium* D (see ref. 6 for lineshape). *Chromatium* D is different from *R. rubrum* and *Rps. spheroides* by virtue of the existence of the irreversible oxidation of cytochrome c_{553} ($E_{m\,7.4} = +10$ mV, ref. 24). The oxidation, which reduces $BChl^+$ is complete after a single flash (2 ms) which, in turn, renders the primary electron acceptor ($E_{m\,7.4} = -135$ mV, ref. 24) irreversibly reduced. In other words, if the detection of the triplet state requires the prior reduction of the primary electron acceptor, then the redox dependence of the flash should be like that seen on steady-state illumination in *R. rubrum* and *Rps. spheroides* (where the involvement with a cytochrome *c* at low temperatures is absent) and should follow the chemical reduction of the primary electron acceptor; the second flash should follow the course of chemical reduction of cytochrome c_{553}.

As shown in Fig. 6, flash-induced triplet is not seen on the initial flash until the primary electron acceptor is reduced with an apparent midpoint potential of -120 mV. On a second flash, however, the triplet signal is formed with an apparent midpoint potential of 10 mV. This effect is caused by the irreversible reduction of the primary electron acceptor effected by the first flash, an effect which is, in turn, caused by the irreversible oxidation of cytochrome c_{553} at potentials below its midpoint [6].

Light saturation

Steady-state triplet amplitude measurements as a function of illumination, show a linear dependence on light intensity up to maximum brightness used in these

experiments. This observation is consistent with a short-lived excited state species which is formed by way of a single photon absorption process. The steady-state g 2.00 signal of oxidized reaction center bacteriochlorophyll, on the other hand, shows linear dependence on light intensity under low intensity illumination, but approaches saturation at higher light levels, implying that the oxidized state of reaction center bacteriochlorophyll is also formed by a one-photon absorption process, but has a much longer lifetime than the triplet state. With flash illumination, the triplet and g 2.00 signals saturate at the same intensity [31].

Kinetic studies

Shown in the lower part of Fig. 7 are a few kinetic traces taken at different magnetic field values. The triplet signal shows a complex decay with a half-time of about 6 μs. A steady-state derivative presentation is shown at the top and an electronically integrated "absorption" signal in the center. It is clear that the kinetically measured triplet signal has essentially an absorption lineshape as expected. As the temperature is increased (above 10 °K), the amplitude of the observed triplet ESR signal becomes smaller and the half-time becomes shorter. Whether this effect is due to more rapid spin-lattice relaxation rates at higher temperatures or due to temperature dependence of triplet state "quenching" is not clear.

Kinetics of the oxidized reaction center bacteriochlorophyll dark re-reduction following flash oxidation are accurately first order and show a time constant of about 30 ms [7, 26]. Thus, since the decay rate of the triplet state is approx. 3000 times more

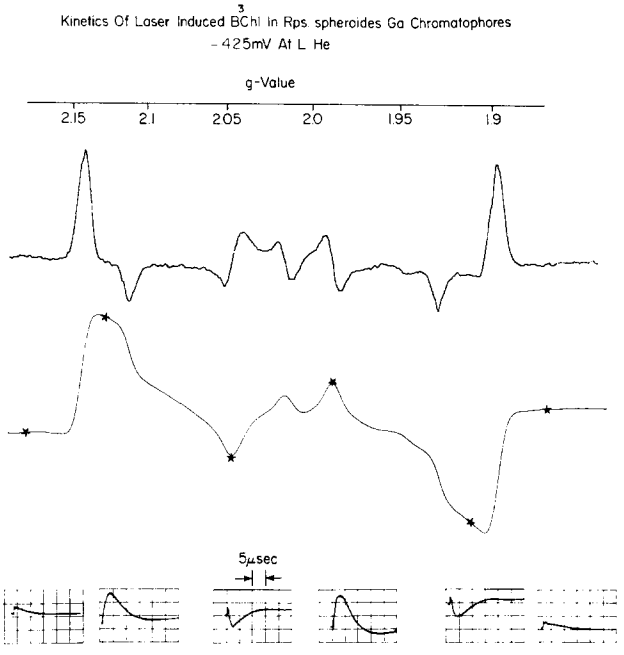

Fig. 7. Triplet kinetics of *Rps. spheroides* Ga mutant at low temperature. Chromatophores from *Rps. spheroides* (Ga) were used at a bacteriochlorophyll concentration of 2 mM. Sample was reduced to a potential of −400 mV, using methyl viologen (100 μM) as a mediator.

rapid, steady-state "saturation" of the triplet state will occur at light intensities approx. 3000 times that for bacteriochlorophyll oxidation, with equal quantum efficiencies of formation.

DISCUSSION

Low-temperature EPR spectra of reaction center triplet states have lineshapes which are composites of microwave absorption and emission. The lineshape of steady-state signals and microsecond kinetic spectra are similar. This demonstrated that entry rates into the triplet manifold are spin selective. Evaluation of the components of spin–orbit coupling between singlet and triplet states show that the non-zero elements involve only the T_0 triplet level. Thus, at temperatures low enough that spin-lattice relaxation rates are slower than triplet state lifetimes, significant spin polarization results. This leads to greatly enhanced EPR signal amplitudes (as much as 200-fold at 10 °K).

With *Rps. spheroides* (R26) reaction center bacteriochlorophyll, fluorescence quantum yield is very low. When the primary electron acceptor is reduced, the measured quantum yield is approx. 10^{-3} [27], implying that, with the acceptor reduced, the lifetime of the excited bacteriochlorophyll singlet state is 20 ps. This time must correspond to the formation of the triplet state, that is, the rate of inter-system crossing (from excited singlet to triplet) must be approx. $5 \cdot 10^{10}\ s^{-1}$. This rate is consistent with a spin–orbit coupling energy of approx. $0.2\ cm^{-1}$. The 3-fold decrease in fluorescence quantum yield in reaction centers in which the acceptor is oxidized, may be accounted for by an increase in spin-orbit coupling to approx. $0.7\ cm^{-1}$.

As previously noted, zero-field splitting parameters D and E in general, arise from both spin–spin and spin–orbit interactions, both of which are sensitive indicators of the geometry and environment of the triplet species. With aromatic π–π^* triplet states, the spin–spin (dipolar) interaction is usually dominant. In fact, if the previous estimate [16] of $0.7\ cm^{-1}$ is assumed for the spin–orbit interaction energy and the lowest lying excited state which mixes effectively with the triplet state is at least $2500\ cm^{-1}$ removed, then the spin–orbit interaction could contribute at most $1 \cdot 10^{-4}\ cm^{-1}$ to D and E. Spin–spin dipolar interactions between two triplet electrons whose average separation is 4.1 Å, give rise to D values of approx. $200 \cdot 10^{-4}\ cm^{-1}$. The magnitude of E is an indicator of deviations from axial symmetry.

The small differences observed in D and E values between different photosynthetic bacteria are most likely related to small differences in average distance between the triplet electrons in the reaction centers. Structural differences are also suggested by the differences in infrared spectral characteristics of the various bacteria. Comparison of the zero-field splitting values with those observed for isolated chlorophylls is consistent with the suggestion that reaction center bacteriochlorophyll is in a dimeric form [28–30].

ACKNOWLEDGEMENTS

The work reported here was supported by National Science Foundation Grant GB-28125 and U.S. Public Health Service Grants GM-12202, and RR-0015.

REFERENCES

1 Livingston, R. (1960) Q. Rev. 14, 174–199
2 White, R. A. and Tollin, G. (1971) Photochem. Photobiol. 14, 15–63
3 Robinson, G. W. (1966) Brookhaven Symp. Biol. 19, 16–44
4 Clayton, R. K. (1965) Molecular Physics in Photosynthesis, pp. 178–191, Blaisdell, New York
5 Franck, J. and Rosenberg, J. L. (1964) J. Theor. Biol. 7, 276
6 Dutton, P. L., Leigh, J. S. and Seibert, M. (1972) Biochem. Biophys. Res. Commun. 46, 406–413
7 Dutton, P. L., Leigh, J. S. and Reed, D. W. (1973) Biochim. Biophys. Acta 292, 654–664
8 Livingston, R., Porter, G. and Windsor, M. (1954) Nature 173, 485–486
9 Pekkarinen, L. and Linschitz, H. (1960) J. Am. Chem. Soc. 82, 2407–2411
10 Bowers, P. G. and Porter, G. (1967) Proc. R. Soc. London, Ser. A, 296, 435
11 Connolly, J. S., Gorman, D. S. and Seeley, G. R. (1973) Am. Soc. Photobiol. WAM-D10, 143
12 Becker, R. S. and Kasha, M. (1955) J. Am. Chem. Soc. 77, 3669–3670
13 Weiss, Jr, C. (1972) J. Mol. Spect. 44, 37
14 Azizova, O. A., Gribova, Z. P., Kayushin, L. P. and Pulatova, M. K. (1966) Photochem. Photobiol. 5, 763–770
15 Lhoste, M. J. M. (1968) Compt. Rend. 266D, 1059–1062
16 Gouterman, M., Yamanoshi, B. S. and Kwiram, A. L. (1972) J. Chem. Phys. 56, 4073–4078
17 Wasserman, E., Snyder, L. C. and Yager, W. A. (1964) J. Chem. Phys. 41, 1763–1772
18 Abragam, A. and Bleaney, B. (1970) Electron Paramagnetic Resonance of Transition Ions, pp. 502–506, Clarendon Press, Oxford
19 Sharnoff, M. (1967) J. Chem. Phys. 46, 3263–3264
20 Kwiram, A. L. (1967) Chem. Phys. Lett. 1, 272
21 Schwoerer, M. and Sixl, A. (1968) Chem. Phys. Lett. 2, 14–19
22 Baltscheffsky, H. (1960) Biochim. Biophys. Acta 40, 1–8
23 Thornber, J. P. (1970) Biochemistry 9, 2688–2698
24 Dutton, P. L. (1971) Biochim. Biophys. Acta 226, 63–80
25 Cramer, W. A. (1969) Biochim. Biophys. Acta 189, 54–59
26 McElroy, J. D., Feher, G. and Mauzerall, D. C. (1969) Biochim. Biophys. Acta 172, 180–183
27 Zankel, K. L., Reed, D. W. and Clayton, R. K. (1968) Proc. Natl. Acad. Sci. U.S. 61, 1243–1249
28 Norris, J. R., Uphaus, R. A., Crespi, H. L. and Katz, J. J. (1971) Proc. Natl. Acad. Sci. U.S. 68, 625–628
29 Norris, J. R., Druyan, M. E. and Katz, J. J. (1973) J. Am. Chem. Soc. 95, 1680–1682
30 Feher, G., Hoff, A. J., Isaacson, R. A. and McElroy, J. D. (1973) Biophys. J. 13, 60a
31 Wraight, C. A., Leigh, J. S., Dutton, P. L. and Clayton, R. K. (1974) Biochim. Biophys. Acta 333, 401–408